Generalized Epidemic Mean-Field Model for Spreading Processes Over Multilayer Complex Networks

Faryad Darabi Sahneh, *Member, IEEE*, Caterina Scoglio, *Member, IEEE*, and Piet Van Mieghem, *Member, IEEE*

***Abstract*—Mean-field deterministic epidemic models have been successful in uncovering several important dynamic properties of stochastic epidemic spreading processes over complex networks. In particular, individual-based epidemic models isolate the impact of the network topology on spreading dynamics. In this paper, the existing models are generalized to develop a class of models that includes the spreading process in multilayer complex networks. We provide a detailed description of the stochastic process at the agent level where the agents interact through different layers, each represented by a graph. The set of differential equations that describes the time evolution of the state occupancy probabilities has an exponentially growing state-space size in terms of the number of the agents. Based on a mean-field type approximation, we developed a set of nonlinear differential equations that has linearly growing state-space size. We find that the latter system, referred to as the *generalized epidemic mean-field* (GEMF) model, has a simple structure characterized by the elements of the adjacency matrices of the network layers and the Laplacian matrices of the transition rate graphs. Finally, we present several examples of epidemic models, including spreading of virus and information in computer networks and spreading of multiple pathogens in a host population.**

***Index Terms*—Complex networks, epidemic spreading, generalized epidemic mean-field (GEMF) model, Markov process, mean field theory.**

I. Introduction

EPIDEMICS are critical phenomena, not only from a biological viewpoint, as infectious diseases, but also from a technological viewpoint, as malware propagation. Clearly, epidemics can produce huge damage, and so the development of accurate and effective models for epidemics is imperative. First, epidemic modeling has a long history in biological systems, and recently, such modeling has attracted substantial attention in modeling propagation phenomena in communication networks [1]–[3]. Epidemic spreading, like many other processes (see, e.g., [4]–[6]) on complex networks, can be modeled as a network of coupled stochastic agents. The population-based or network-based epidemic models (cf., [7]–[9]) extended to individual-based epidemic models [10]–[14]. A common approach of existing individual-based models is to consider Markovian interacting agents (i.e., dynamics of the agents satisfy the Markov property [15], [16]), while the interaction is represented by a generic graph. This approach avoids random network models (e.g., Erdös–Réyni [17], Barábasi–Albert [18], etc.), which may fail to properly represent engineered networks [19].

The study of the dynamic behavior of epidemic spreading processes on graphs is very challenging, even for simple scenarios, due to the stochastic nature of this behavior. For example, the system governing state occupancy probabilities has an exponentially growing space size in terms of the number of the agents. Therefore, the problem becomes soon intractable as the number of agents increases. Fortunately, through a mean-field closure approximation approach, the size of the governing equations reduces dramatically although at the expense of exactness. Mean-field epidemic models have been very successful in finding several interesting results for individual-based epidemic spreading processes. For example, researchers have shown that the epidemic threshold in the Susceptible-Infected-Susceptible (SIS) model is actually the inverse of the spectral radius of the adjacency matrix of the contact graph [10], [12].

In most existing individual-based epidemic models, the interaction is driven by a single graph. However, studying epidemics in communication networks and cyber-physical systems requires a more elaborate description of the interaction. Several researchers from computer science, communication, networking, and control communities are working on describing this complex interaction by using multiple interconnected networks [20]–[22]. Ultimately, the study of the spreading of epidemics in interconnected networks is a major challenge of complex networks [23]–[27].

In this paper, we provide a novel and generalized formulation of the epidemic spreading problem and a modeling solution. We consider a spreading process among a group of agents that can be in M different compartments and where the agents interact through a multilayer network, which is explained in detail in Section IV. We follow a rigorous methodology to develop a general epidemic spreading model. The modeling starts with a simple agent-level description of the underlying stochastic process. The exact Markov equations, which describe the time evolution of the state occupancy probabilities, are linear differential equations, however, with exponentially growing state-space size in terms of the number of agents. Through a

Manuscript received April 05, 2012; revised September 22, 2012; accepted November 12, 2012; approved by IEEE/ACM TRANSACTIONS ON NETWORKING Editor Y. Liu. Date of publication January 29, 2013; date of current version October 11, 2013. This work was supported by the National Agricultural Biosecurity Center at Kansas State University.

F. Darabi Sahneh and C. Scoglio are with the Electrical and Computer Engineering Department, Kansas State University, Manhattan, KS 66506 USA (e-mail: faryad@ksu.edu; caterina@ksu.edu).

P. Van Mieghem is with the Faculty of Electrical Engineering, Mathematics and Computer Science, Delft University of Technology, 2600 GA Delft, The Netherlands (e-mail: P.F.A.VanMieghem@tudelft.nl).

Color versions of one or more of the figures in this paper are available online at http://ieeexplore.ieee.org.

Digital Object Identifier 10.1109/TNET.2013.2239658

mean-field type approximation, the state space dramatically reduces. The approximate system is a set of nonlinear ordinary differential equations that we call the generalized epidemic mean-field (GEMF) model. We apply GEMF to interesting problems, such as: 1) the spread of infection in a population where the infection spreads through a contact network while agents respond to the spreading by learning about the existence of the infection through information dissemination networks, and 2) the bi-spreading of two types of interacting viruses in a host population demanding different transmission routes for the infection propagation.

The contribution of this paper is twofold. First, we propose a general epidemic-like spreading Markov model with multi-compartment agent dynamics and a multilayer interaction network. Second, we propose GEMF as a generalized epidemic mean-field model suitable for a large class of individual-based spreading scenarios. GEMF is rigorously derived from an agent-level description of the spreading process and is elegantly expressed [see (26)] in terms of the adjacency matrix of each network layer and of the Laplacian of the transition rate diagrams. In GEMF, there is no approximation of the network topology; the only approximation is a mean-field type approximation of the dynamics of the agents. The impact of this approximation is a function of the network topologies and epidemic parameters. For complete development, we have also explicitly derived the exact Markov equations in the Appendix.

The rest of the paper is organized as follows. Motivations for developing GEMF are provided in Section II through examples, and Section III offers the basic definitions for the spreading problem. In Section IV, the agent-level Markov description of the spreading process is provided, and GEMF is developed in Section V. The paper concludes in Section VI by applying GEMF to some existing and novel spreading scenarios.

II. Motivating Examples

In this section, first we review some of the existing individual-based epidemic models, and at the end, we discuss what generalizations are important to develop a general class of epidemic models.

A. SIS Individual-Based Model

In the SIS model (cf., [11]–[13]), each agent can be either "*susceptible*" or "*infected*." Hence, the number of compartments, denoted by M, in the SIS model is $M = 2$. A susceptible agent can become infected if it is surrounded by infected agents. The infection process of an agent with one infected neighbor is a Poisson process with transition rate β. The infection processes are stochastically independent of each other. Therefore, for a susceptible agent with more than one infected agent in its neighborhood, the transition rate is the infection rate β times the number of the infected agents. The neighborhood of each agent is determined by a graph $\mathcal{G}_c$, which represents the *contact network*. In addition to the infection process, there also exists a curing process. An infected agent becomes susceptible with a curing rate δ. A schematic for the SIS model is shown in Fig. 1.

B. SAIS Spreading Model

The Susceptible-Alert-Infected-Susceptible (SAIS) model was developed in [28] to incorporate agent reactions to the spread of the virus. In the SAIS spreading model, each agent

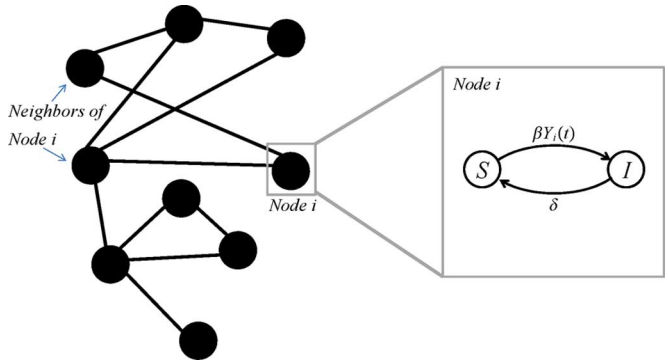

Fig. 1. Schematic of a contact network along with the agent-level stochastic transition diagram for agent i according to the SIS epidemic spreading model (explained in Section II-A). The parameters β and δ denote the infection rate and curing rate, respectively. $Y_i(t)$ is number of the neighbors of agent i that are infected at time t.

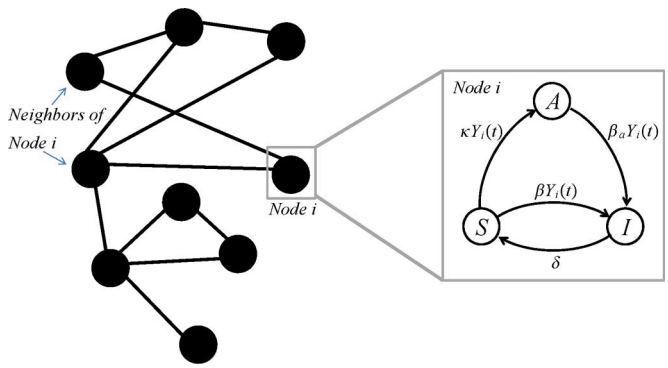

Fig. 2. As in Fig. 1, the SAIS epidemic is sketched (see Section II-B) on a contact network G_c. In addition to the infection rate β and the curing rate δ, parameters β_a and κ denote the alerted infection rate and the alerting rate, respectively. $Y_i(t)$ is the number of neighbors of agent i that are infected at time t.

can be either "*susceptible*," "*infected*," or "*alert*." Hence, the number of compartments in the SAIS model is $M = 3$. The curing process in SAIS is the same as the curing process in the SIS model and is characterized by curing rate δ. The infection process of a susceptible agent is also similar to that of the SIS model, which is determined by infection rate β and contact graph $\mathcal{G}_c$. However, in the SAIS model, a susceptible agent can become alert if it senses infected agents in its neighborhood. In the SAIS model, the alerting transition rate is κ times the number of infected agents. An alert agent can also become infected by the process similar to the infection process of a susceptible agent. However, the infection rate for alert agents is lower due to increased security for computer networks or better hygiene in the human population. The alert infection rate is denoted by $\beta_a < \beta$. Fig. 2 is a schematic for the SAIS spreading model.

C. Generalization of Epidemic Models

The SIS and SAIS models are good examples of how a simple compartmental model at the node level along with a network topology can lead to very rich and complex dynamics. While following the structure and underlying assumptions of these existing epidemic models, we propose to develop a generalized individual-based spreading model where: 1) the node model has

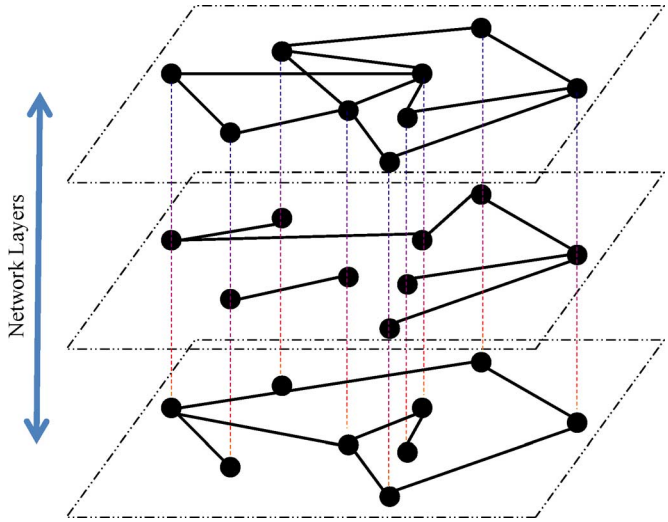

Fig. 3. Network layers describe the different types of interactions among agents in GEMF. The vertical dotted lines emphasize that all graphs have the same nodes, but the edges are different.

multiple compartments; and 2) the network topology has multiple layers. Both generalizations are important. For example, many epidemic models can be created by adding new compartments to the basic SIS or SIR epidemic models. Also, for applications in cyber-social and cyber-physical systems, more network layers need to be taken into account (see Fig. 3). For example, in the SAIS model, the agents can observe the infection status of their neighbors in the contact network. However, a more realistic scenario is that agents learn about the infection status of other agents through an *infection information dissemination network*, represented by $\mathcal{G}_{\text{iIDN}}$, which can be very different from the contact network. We can also take into account an *alert information dissemination network* among the agents, represented by $\mathcal{G}_{\text{aIDN}}$. Through this network, agents can become alert if some of their neighbors (determined by $\mathcal{G}_{\text{aIDN}}$) are alert. In this case, the network topology has three layers. In Section VI-C, we develop an SAIS model with information dissemination.

Multilayer epidemic modeling can also have applications in biological networks. Consider the scenario where two pathogens are spreading through the host population. Infection by one pathogen can effectively influence the infection process by the other pathogen. Since the infection transmission routes may be different, the contact networks for each virus can potentially be separate from each other. In Section VI-D, we develop an individual-based SIS bi-spreading model with separate contact networks for each pathogen.

The GEMF class of models developed in this paper allows not only an arbitrary number of compartments, but also accounts for multiple network layers.

III. Definitions

The network consists of N interacting agents, each of which can be in one of M states (compartments). The stochastic transitions of an agent not only depend on its own state, but also on the states of the other agents. The group of agents is assumed to be *jointly Markovian*, i.e., the collective system is a Markov process. The state of the collective system, which we refer to as the network state, is actually the joint state of all the agents' states. Assuming that all the agents can take values among M compartments, the size of the network state space is M^N. In Section III-A, the agent state and network state are precisely defined.

A. Agent State and Network Markov State

One of the generalizations of GEMF concerns the compartment set, where each agent can be in one compartment in the set $\mathcal{S} = \{s_1, s_2, \ldots, s_m, \ldots, s_M\}$. For example, in the SIS model for epidemic spread, $M = 2$ and $\mathcal{S} = \{\text{`}Susceptible\text{'}, \text{`}Infected\text{'}\}$. From now on, without loss of generality, each compartment is labeled with a number from 1 to M. The *agent state* $x_i(t)$ of agent i at time t is $x_i(t) = e_m$ if the agent i is in compartment m at time t. Here, e_m is the mth standard unit vector in the $\mathbb{R}^M$ Euclidean space, i.e., all entries of e_m are zero except for the mth entry, which is equal to one

$$e_m \triangleq [0 \ldots 0 \underbrace{1}_{m\text{th entry}} 0 \ldots 0]^T \in \mathbb{R}^M. \tag{1}$$

The definition $x_i(t) = e_m$ illustrates that each entry of $x_i(t)$ is a Bernoulli random variable. Therefore, the expected value of $x_i(t)$ is in fact the *compartment occupancy probability vector*, i.e.,

$$E[x_i] = [\Pr[x_i = e_1], \ldots, \Pr[x_i = e_M]]^T. \tag{2}$$

The above property is very important in future developments, particularly in (14), (17), and (24)–(26).

There are other possibilities for defining the node state $x_i(t)$. For example, one might define $x_i = m - 1$ if node i is in compartment m. By this definition, x_i takes values from 0 to $M - 1$. This definition is particularly useful if $M = 2$. In this case, x_i is a binary random variable. Van Mieghem *et al.* [12] used this definition for the SIS N-Intertwined model.

As stated, the dynamics of an individual agent depend on the states of the other agents. Therefore, the state of a single agent is not enough to describe the evolution of the agent state. Instead, the joint state of all the agents follows a Markov process. Therefore, the *network state* at time t, denoted by $X(t)$, is the joint state of all the agents defined as [29]

$$X(t) = \bigotimes_{i=1}^{N} x_i(t) = x_1(t) \otimes x_2(t) \otimes \cdots \otimes x_N(t) \tag{3}$$

where $\otimes$ is the Kronecker product.

By (3), $X(t)$ is an $M^N \times 1$ random vector with exactly one element equal to one and the rest equal to zero. Therefore, the expected value of $X(t)$ is the joint probability distribution function of the network state. For example, for the SIS model, the first element of the expectation of $X(t)$ is the probability that all the agents are simultaneously susceptible.

One could define the network state as an $MN \times 1$ vector $X \triangleq [x_1^T, x_2^T, \ldots, x_N^T]^T$. However, in this case, the expectation of $X(t)$ will only provide the marginal probability distribution of the node states. As Section V-A shows, the information about marginal probabilities at a given time is not enough to describe the evolution of the marginal probabilities, and the joint probability distribution is required. Hence, we adopt definition (3) for the network state.

B. Multilayer Network Topology

The other generalization in GEMF concerns the topology. In most epidemic models, the interaction among the agents is represented by the contact network. However, as discussed in Section II-C, the types of interaction can be different in a complex network. For our modeling purpose, we represent the topology by L layers of graphs $\mathcal{G}_l(\mathcal{N}, E_l)$, where $\mathcal{N}$ is the set of nodes denoting the agents, and E_l is the set of edges that represent the interaction between each pair of individuals in the lth layer. These graphs have the same nodes, but the edges can be different. The adjacency matrix corresponding to graph $\mathcal{G}_l$ is denoted by $\mathcal{A}_l = [a_{l,ij}]_{N\times N}$. If agent j can *influence* agent i in the layer l, $a_{l,ij} = 1$, otherwise $a_{l,ij} = 0$. In Section IV-A.2, we define precisely what "influence" implies in our model. A representation of the network layering structure is depicted in Fig. 3.

IV. Agent-Level Description of the Markov Spreading Process

The network state $X(t)$ follows a continuous-time Markov process. Knowing that the network is in state $X(t)$ at time t, what is the network state $X(t+\Delta t)$ at time $t+\Delta t$? In a network of interacting agents, this question can be very complicated. Instead, a more direct approach is to describe the agent state $x_i(t+\Delta t)$ given the network state $X(t)$ at time t. The spreading process is fully described if the probability to record a transition from compartment m to compartment n for agent i, conditioned on the network state $X(t)$, is known for all possible values of m, n, and i. Therefore, in this section, we focus on deducing an expression for $\Pr[x_i(t+\Delta t) = e_n \,|\, x_i(t) = e_m, X(t)]$, which will be used later to develop the GEMF model. The challenge in deducing an expression for $\Pr[x_i(t+\Delta t) = e_n \,|\, x_i(t) = e_m, X(t)]$ is that too many possibilities exist for the dependence of the transition $m \to n$ of the individual agent i on the network state. Here are a few examples: the transition $m \to n$ happens completely independently from the states of other agents; the transition $m \to n$ happens if the number of other agents in compartment m are more than the number of agents in compartment n; the transition $m \to n$ happens if agents 1 and 2 are both in compartment m and the rate of the transition is the logarithm of the number of agents in compartment m. All of these examples are legitimate so far. However, we need to specify the transition possibilities properly to develop a coherent and consistent epidemic spreading model.

A. Epidemic Spreading Process Modeling

The SIS model (see Section II-A) gives very good insights into how to properly define the transition possibilities to describe an epidemic spreading process. In the SIS model, there are two transitions. The curing process, which is basically the transition from "*infected*" state to "*susceptible*," occurs independently of the states of other agents. Instead, the infection process, which refers to transition from "*susceptible*" state to "*infected*" state, happens through a different mechanism. A susceptible agent is in contact with some other agents, and during the time interval $(t, t+\Delta t]$, the susceptible agent receives the infection from its infected neighbor with some probability. The process of receiving the infection from one infected neighbor is independent of the process of receiving the infection from another neighbor. Indeed, all the infected neighbors compete to infect the susceptible agent. The susceptible agent becomes infected when one of the neighbors succeeds transmitting the infection. Next, since the transitions in the SIS epidemic model are very similar to the transitions in most existing epidemic models, we impose a similar structure of independent competing processes to the generalized spreading model.

Assumption 1: A transition $m \to n$ for agent i is the result of several stochastically independent competing processes: the process $m \to n$ for agent i that happens independently of the states of other agents, and the process $m \to n$ for agent i because of interaction with agent $j \neq i$, for each $j \in \{1, \ldots, N\} \backslash \{i\}$.

According to Assumption 1, the interaction of agent i with agent $j \neq i$ is stochastically independent of its interaction with agent $k \notin \{i, j\}$. Next, define the auxiliary counting process $T_{(i,j)}^{m\to n}(t)$ corresponding to the interaction of agent i with agent j. For convenience of notations, let $T_{(i,i)}^{m\to n}(t)$ correspond to the transition for agent i occurring independently of the states of other agents. According to Assumption 1, conditioned on the network state, these counting processes are stochastically independent. The transition $m \to n$ occurs in the time interval $(t, t+\Delta t]$ if any of these counting processes records an event. Therefore, $\Pr[x_i(t+\Delta t) = e_n \,|\, x_i(t) = e_m, X(t)]$ can be written as

$$\begin{aligned}\Pr[x_i(t+\Delta t) = e_n \,|\, x_i(t) = e_m, X(t)] \\ = \Pr\Big[\exists j \in \{1, \ldots, N\} \text{ s.t. } T_{(i,j)}^{m\to n}(t+\Delta t) \\ - T_{(i,j)}^{m\to n}(t) \neq 0 \,|\, X(t)\Big]. \end{aligned} \quad (4)$$

Each of the counting processes $T_{(i,j)}^{m\to n}(t)$ is a Poisson process with the rate $\lambda_{(i,j)}^{m\to n}(t)$, to be determined. Therefore

$$\begin{aligned}\Pr\Big[T_{(i,j)}^{m\to n}(t+\Delta t) - T_{(i,j)}^{m\to n}(t) \neq 0 \,|\, X(t)\Big] \\ = \lambda_{(i,j)}^{m\to n}(t)\Delta t + o(\Delta t). \end{aligned} \quad (5)$$

The sum of independent Poisson processes is also a Poisson process with aggregate rate equal to the sum of the individual rates (see [16, Theorem 7.3.4]). Therefore

$$\begin{aligned}\Pr[x_i(t+\Delta t) = e_n \,|\, x_i(t) = e_m, X(t)] \\ = \Delta t \sum_{j=1}^{N} \lambda_{(i,j)}^{m\to n}(t) + o(\Delta t). \end{aligned} \quad (6)$$

The remaining part of this section is to determine $\lambda_{(i,j)}^{m\to n}(t)$ properly. For this end, we define notions of nodal and edge-based transitions.

1) Nodal Transition: As discussed earlier in Section II-A, the curing process in SIS model happens with rate δ regardless of the infection status of other agents. Correspondingly, we call a process that occurs independently of the states of other agents a *nodal transition*. In general, for the nodal transition $m \to n$, we can consider a rate[1] $\delta_{mn} \geq 0$, which is actually the rate for the counting process $T_{(i,i)}^{m\to n}(t)$, i.e.,

$$\lambda_{(i,i)}^{m\to n}(t) = \delta_{mn}. \quad (7)$$

[1]Here, δ_{mn} is a nonnegative scalar that represents nodal transitions. It should not be confused with the Kronecker delta symbol.

2) Edge-Based Transition: In the SIS model, a susceptible agent i becomes infected with rate β if it is in contact with infected agent j. Correspondingly, we call a process that occurs as the result of interaction between a pair of agents an *edge-based transition*. Edge-based transitions are different from nodal transitions because they depend on the states of other agents. For example, in the SIS model, the infection process is an edge-based transition, where the contact network graph determines the contact among agents. However, as described in Section III-B, we extend the concept of contact network to multilayer networks. In our formulation, the interactions among agents consist of L graph layers. Corresponding to each layer l, there is one *influencer compartment* q_l, i.e., transition $m \to n$ can occur for agent i as the result that a neighbor j in layer l, i.e., $a_{l,ij} = 1$, is in q_l. For example, in the SIS model, "*infected*" is the influencer compartment for the contact network, i.e., $q_1 = 2$. In general, the transition from compartment m to n is characterized by the transition rate $\beta_{l,mn} \geq 0$ for layer l. Therefore, the edge-based transition from m to $n \neq m$ through interaction of agent i with agent j is described by the rate

$$\lambda_{(i,j)}^{m \to n}(t) = \sum_{l=1}^{L} \beta_{l,mn} a_{l,ij} 1_{\{x_j(t) = e_{q_l}\}} \tag{8}$$

where $1_{\{\cdot\}}$ is the indicator function.

It is possible that the influencer compartment of two distinct layers is the same. For example, recall the extended SAIS model with three network layers proposed in Section II-C. For the contact network and the infection information dissemination network, "*infected*" is the influencer compartment. However, for the alert information dissemination network, "*alert*" is the influencer compartment.

Assigning only one influencer compartment to a graph layer allows the elegant development of the subsequent analysis. However, a more general possibility is that a transition $m \to n$ occurs if a neighbor j, i.e., $a_{l,ij} = 1$, is in a subset of the compartments, say $q_{l,1}$ or $q_{l,2}$. This case can be treated within the same structure of GEMF, and if so, we can count the network layer twice, i.e., we assume that the first time, the graph has the influencer compartment $q_{l,1}$, and the second time, the graph has the influencer compartment $q_{l,2}$. An example of this case is in Section VI-D.

B. Transition Rate Graphs

To make the subsequent developments systematic, we propose to use transition rate graphs defined as follows. A *nodal transition rate graph* is graph with M nodes, where each node represents a compartment. A directed link (m, n) from m to n represents the nodal transition $m \to n$ weighted by the positive transition rate $\delta_{mn} > 0$. Corresponding to the nodal transition rate graph, the adjacency matrices of the nodal transition rates A_δ is

$$A_\delta \triangleq [\delta_{mn}]_{M \times M}. \tag{9}$$

An *edge-based transition rate graph*, corresponding to the network layer $\mathcal{G}_l$, is a graph with M nodes where each node represents a compartment. A directed link (m, n) from m to n represents the edge-based transition $m \to n$ weighted by the positive transition rate $\beta_{l,mn} > 0$ in network layer l with influencer compartment q_l. Corresponding to the edge-based transition rate graph, the adjacency matrices of the edge-based transition rates A_{β_l} are

$$A_{\beta_l} \triangleq [\beta_{l,mn}]_{M \times M}. \tag{10}$$

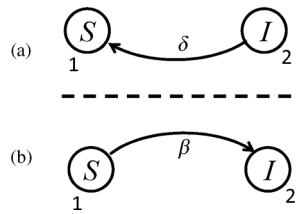

Fig. 4. Transition rate graphs in the SIS model. (a) Nodal transition rate graph. Nodes represent the two compartments "*susceptible*" and "*infected*." Directed link from I to S represents curing process (a nodal transition) weighted by the curing rate $\delta > 0$. (b) Edge-based transition graph of the contact network layer $\mathcal{G}_c$. Directed link from S to I represents the infection process (edge-based transition) weighted by the infection rate $\beta > 0$. For the contact network, the influencer compartment is $q_1 = 2$, i.e., "*infected*."

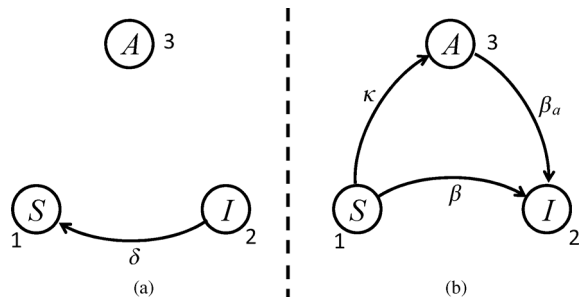

Fig. 5. Transition rate graphs in the SAIS model. (a) Nodal transition rate graph. Nodes represent the three compartments "*susceptible*," "*infected*," and "*alert*." Directed link from I to S represents curing process (a nodal transition) weighted by the curing rate $\delta > 0$. (b) Edge-based transition graph of the contact network layer $\mathcal{G}_c$. Directed link from S to I represents the infection process (edge-based transition) weighted by the infection rate $\beta > 0$. Directed link from S to A represents the alerting process (edge-based transition) weighted by the alerting rate $\kappa > 0$. Directed link from A to I represents the alerted infection process (edge-based transition) weighted by the alerted infection rate $\beta_a > 0$. For the contact network, the influencer compartment is $q_1 = 2$, i.e., "*infected*."

For example, in both the SIS and SAIS models described in Sections II-A and II-B, only the curing process is a nodal transition. The nodal transition rate graphs for the SIS and SAIS models are shown in Figs. 4 and 5, respectively. The schematic of the nodal transition rate graph in general is drawn in the left-hand side of Fig. 6. In both the SIS and SAIS models, the contact network is the only network layer. Therefore, they have one edge-based transition rate graph. The edge-based transition rate graphs for the SIS and SAIS models are shown in Figs. 4 and 5, respectively. The schematic of the transition rate graphs in general is drawn in the right-hand side of Fig. 6.

In Section V [see (26)], the Laplacian matrices (see [30]) associated to the transition rate graphs appears in the expression of GEMS.

C. Agent-Level Markov Description of the Spreading Process

In Section IV-A, we developed the expressions for the nodal transition and edge-based transitions. Substituting (7) and (8) into (6) yields

$$\begin{aligned} &\Pr[x_i(t + \Delta t) = e_n \,|\, x_i(t) = e_m, X(t)] \\ &\qquad = \delta_{mn} \Delta t + \Delta t \sum\nolimits_{l=1}^{L} \beta_{l,mn} y_{l,i}(t) + o(\Delta t) \end{aligned} \tag{11}$$

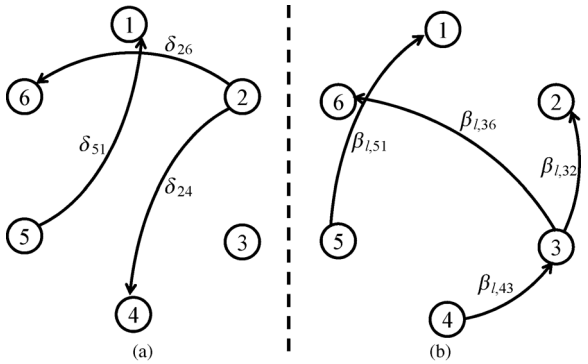

Fig. 6. Transition rate graphs in GEMF. (a) Nodal transition rate graph. Nodes represent compartments. Directed link (m, n) represents nodal transition $m \to n$ weighted by the transition rate $\delta_{mn} > 0$. (b) Edge-based transition graph of network layer $\mathcal{G}_l$. Directed link (m, n) represents the edge-based transition $m \to n$ weighted by the transition rate $\beta_{l,mn} > 0$ in network layer l. The inducer compartment of layer l is q_l.

for $i = \{1, \ldots, N\}$ and $m \neq n$, where

$$y_{l,i}(t) \triangleq \sum_{j=1}^{N} a_{l,ij} 1_{\{x_j(t)=e_{q_l}\}} \tag{12}$$

is the number of neighbors of agent i in $\mathcal{G}_l$ that are in the corresponding influencer compartment q_l.

Equation (11) provides an agent-level description of the Markov process. It can be used directly for Monte Carlo numerical simulation of the spreading process.

V. Generalized Epidemic Mean-Field Model

The objective of this section is to derive the time evolution of the state occupancy probabilities.

A. Exact Markov Differential Equation

In Section IV, the spreading model was described, and the corresponding Markov process was derived in (11). The evolution of the state occupancy probabilities associated with a Markov process follows a set of differential equations known as the Kolmogorov differential equations. The derivation of the Kolmogorov differential equation of a Markov process is fairly standard (see [16] and [31]) when the transition rates between the states of the Markov process are known. However, the challenge here is that the network states are the actual Markov states, and instead of the transition rates between the network states, we have the agent-level description of the transitions in (11). Thus, in this section, we derive the differential equations directly from (11).

According to (11), the probability of remaining in the previous state is

$$\begin{aligned}\Pr[x_i(t+\Delta t) = e_m \,|\, x_i(t) = e_m, X(t)] \\ = 1 - \sum_{n \neq m} \Pr[x_i(t+\Delta t) = e_n \,|\, x_i(t) = e_m, X(t)].\end{aligned} \tag{13}$$

Combining (2), (11), and (13) leads to

$$\begin{aligned}&E[x_i(t+\Delta t) \,|\, x_i(t) = e_m, X(t)] \\ &= \begin{bmatrix} \delta_{m1} + \sum_{l=1}^{L} \beta_{l,m1} y_{l,i}(t) \\ \vdots \\ \delta_{m(m-1)} + \sum_{l=1}^{L} \beta_{l,m(m-1)} y_{l,i}(t) \\ -\tilde{\delta}_{mm} - \sum_{l=1}^{L} \tilde{\beta}_{l,mm} y_{l,i}(t) \\ \delta_{m(m+1)} + \sum_{l=1}^{L} \beta_{l,m(m+1)} y_{l,i}(t) \\ \vdots \\ \delta_{mM} + \sum_{l=1}^{L} \beta_{l,mM} y_{l,i}(t) \end{bmatrix} \\ &\quad \times \Delta t + e_m + \epsilon(\Delta t)\end{aligned} \tag{14}$$

where $\tilde{\delta}_{mm} \triangleq \sum_{n \neq m} \delta_{mn}$, $\tilde{\beta}_{l,mm} \triangleq \sum_{n \neq m} \beta_{l,mn}$, and $\epsilon(\Delta t)$ is a function of higher-order terms of Δt satisfying the condition

$$u^T \epsilon(\Delta t) = 0 \tag{15}$$

where u is the all ones vector with appropriate dimensions.

Next, we define the generalized transition matrices $Q_\delta \in \mathbb{R}^{M \times M}$ and $Q_{\beta_l} \in \mathbb{R}^{M \times M}$ with the elements

$$\begin{aligned}(Q_\delta)_{mn} &\triangleq -\delta_{mn} \quad (Q_{\beta_l})_{mn} \triangleq -\beta_{l,mn}, m \neq n \\ (Q_\delta)_{mm} &\triangleq \sum_{n \neq m} \delta_{mn} \quad (Q_{\beta_l})_{mn} \triangleq \sum_{n \neq m} \beta_{l,mn}.\end{aligned} \tag{16}$$

According to definitions (16), the matrices Q_δ and Q_{β_l} are actually the Laplacian matrices of transition rate graphs defined in Section IV-B.

Using (14) and the definition (16), $E[x_i(t+\Delta t) \,|\, X(t)]$ is

$$\begin{aligned}E[x_i(t+\Delta t) \,|\, X(t)] = &-Q_\delta^T x_i(t) \Delta t \\ &- \sum_{l=1}^{L} y_{l,i}(t) Q_{\beta_l}^T x_i(t) \Delta t \\ &+ x_i(t) + \epsilon(\Delta t)\end{aligned} \tag{17}$$

where $y_{l,i}(t)$ is defined in (12). Computing the expected value of each side of (17), we get

$$\begin{aligned}E[x_i(t+\Delta t)] = &-Q_\delta^T E[x_i(t)] \Delta t \\ &- \sum_{l=1}^{L} Q_{\beta_l}^T E[y_{l,i}(t) x_i(t)] \Delta t \\ &+ E[x_i(t)] + \bar{\epsilon}(\Delta t)\end{aligned} \tag{18}$$

where $\bar{\epsilon}(\Delta t) = E[\epsilon(\Delta t)]$ and we have used the formula for iterative expectation (see [32]) rule $E[E[X \,|\, Y]] = E[X]$ to find $E[x_i(t+\Delta t)]$. Moving the $E[x_i(t)]$ term in (18) to the left side and dividing both sides by Δt yields

$$\begin{aligned}&\frac{E[x_i(t+\Delta t)] - E[x_i(t)]}{\Delta t} \\ &= -Q_\delta^T E[x_i(t)] - \sum_{l=1}^{L} Q_{\beta_l}^T E[y_{l,i}(t) x_i(t)] + \frac{1}{\Delta t} \bar{\epsilon}(\Delta t).\end{aligned} \tag{19}$$

Letting $\Delta t \to 0$ in (19), we obtain

$$\frac{d}{dt} E[x_i(t)] = -Q_\delta^T E[x_i(t)] - \sum_{l=1}^{L} Q_{\beta_l}^T E[y_{l,i}(t) x_i(t)]. \tag{20}$$

Furthermore, according to (12), the term $E[y_{l,i}(t)x_i(t)]$ in (20) can be written as

$$E[y_{l,i}(t)x_i(t)] = \sum_{j=1}^{N} a_{l,ij} E[(x_j)_{q_l} x_i(t)]. \tag{21}$$

The term $E[(x_j)_{q_l} x_i(t)]$ in (21) is actually embedded in $E[x_i(t) \otimes x_j(t)]$. Therefore, the evolution of $E[x_i(t)]$ depends on the $E[x_i(t) \otimes x_j(t)]$ term, which is the joint state of pairs of nodes. This means that the marginal information about the compartmental occupancy probabilities is not enough to fully describe the time evolutions of the marginal probabilities. If we continue to derive the evolution law for $E[x_i(t) \otimes x_j(t)]$, it turns out that the time derivative of $E[x_i(t) \otimes x_j(t)]$ depends on terms of the form $E[x_i(t) \otimes x_j(t) \otimes x_k(t)]$, which are the joint states of triplets. This dependency of the evolution of expectation of K-node groups upon expectation of $(K+1)$-node groups continues until K reaches $K = N$. As a result, any system describing the evolution of the expected value of the joint state of any group of $K < N$ nodes is not a closed system. When $K = N$, the expectation of the joint state of all nodes $E[x_1(t) \otimes \cdots \otimes x_N(t)]$, which according to definition (3) is actually the expectation of the network state, satisfies a differential equation of the form

$$\frac{d}{dt} E[X] = -\mathbf{Q}^T E[X] \tag{22}$$

where $\mathbf{Q} \in \mathbb{R}^{M^N \times M^N}$ is the infinitesimal generator (see [16] and [31]) of the underlying Markov process. The Kolmogorov differential equation (22), which we refer to as the exact Markov model, is derived explicitly in the Appendix.

The exact Markov equation (22) fully describes the system. However, the above differential equation has M^N states. Therefore, for large values of N, it is neither analytically nor computationally tractable. Section V-B shows that through a *mean-field type approximation*, a differential equation with MN states can be derived.

B. GEMF

One way to reduce the M^N state-space size is to use closure approximation techniques. As explained in Section V-A, expectations of order K depend on expectation of order $K+1$. The goal of closure techniques is to *approximate* the expectations of order $K+1$ and express them in terms of expectations of order less than or equal to K. In this way, a new set of differential equations is obtained that is closed and has the state-space size $M^K \binom{N}{K}$, which is polynomially growing by N. The simplest approximation is the mean-field type approximation [33]. In first-order mean-field models [12], the states of nodes are assumed to be independent random variables. It is also possible to consider higher-order mean-field approximations. Cator and Van Mieghem [34] used a second-order mean-field approximation and found more accurate performance of the model. Another approach is called the *moment closure* technique, where the joint states of triplets are assumed to have a specific distribution (usually normal or lognormal) [11], [33]. In this way, the joint expectation of triplets is expressed in terms of expectations of pairs. Taylor *et al.* [33] have compared the performances of different approximations.

In this paper, we use a first-order mean-field type approximation. Using this approximation, the joint expected values are approximated in terms of marginal expected values. Specifically, the term $E[(x_j)_{q_l} x_i(t)]$ in (21) is approximated by

$$E[(x_j)_{q_l} x_i(t)] \simeq (E[(x_j)_{q_l}]) E[x_i(t)]. \tag{23}$$

This approximation assumes independence among the random variables. Using the approximation (23), we can describe the time evolution of the expected values through a set of ordinary differential equations with MN states.

We can denote by $v_i(t)$, the expected value of x_i at time t, i.e.,

$$v_i(t) \triangleq E[x_i(t)]. \tag{24}$$

Substituting $E[y_{l,i}(t)x_i(t)] = \sum_{j=1}^{N} a_{l,ij} (v_j(t))_{q_l} v_i(t)$ in (20), from (21), (23), and (24), yields

$$\frac{d}{dt} v_i(t) = -Q_\delta^T v_i(t) - \sum_{l=1}^{L} Q_{\beta_l}^T \sum_{j=1}^{N} a_{l,ij} (v_j(t))_{q_l} v_i(t). \tag{25}$$

Arranging the terms in (25) specifies our generalized epidemic mean-field model GEMF

$$\frac{dv_i}{dt} = -Q_\delta^T v_i - \sum_{l=1}^{L} \left(\sum_{j=1}^{N} a_{l,ij} v_{j,q_l} \right) Q_{\beta_l}^T v_i, \quad i = \{1, \ldots, N\}. \tag{26}$$

Having initially $u^T v_i(t_0) = 1$, the sum of the probabilities is guaranteed to be 1 at any time. The reason is that, from (26), $u^T v_i$ does not change over time because

$$\begin{aligned} \frac{d}{dt} u^T v_i &= -u^T Q_\delta^T v_i - \sum_{l=1}^{L} \left(\sum_{j=1}^{N} a_{l,ij} v_{j,q_l} \right) u^T Q_{\beta_l}^T v_i \\ &= -(Q_\delta u)^T v_i - \sum_{l=1}^{L} \left(\sum_{j=1}^{N} a_{l,ij} v_{j,q_l} \right) (Q_{\beta_l} u)^T v_i \\ &= \mathbf{0}. \end{aligned} \tag{27}$$

The last conclusion is for the fact that $Q_\delta u = 0$ and $Q_{\beta_l} u = 0$, since indeed Q_δ and Q_{β_l} are the graph Laplacians for which u is the eigenvector corresponding to a zero eigenvalue.

GEMF has a systematic procedure to develop different spreading mean-field models. For any specific scenario, the compartment set, the network layers, and their corresponding influencer compartments should be identified, and the transition rate graphs should be drawn. Next, the individual-based mean-field model of the spreading scenario is found by plugging the matrices Q_δ and Q_{β_l}, obtained from the transition rate graphs, into GEMF (26).

C. Capabilities and Limitations of GEMF

GEMF can be used to describe a wide range of spreading scenarios in a systematic way. In part, this is because in GEMF, there is no approximation of the underlying networks. The only approximation belongs to the mean-field-type approximation (23), and how much this results in deviation from exactness is outside the scope of this paper. However, the available studies

for the mean-field SIS model (see [35] and [36]) can shed some light on this problem. Concerning the SIS model, extensive numerical simulations have shown that for sparser graphs, the mean-field model is less accurate, while for graphs with more mixing, the mean-field model is closer to the exact process. For a homogeneous mixing contact network, it has been proved that the mean-field model is asymptotically exact, i.e., as $N \to \infty$. Furthermore, the accuracy of the mean-field model very much depends on the range of the epidemic parameters. For example, in the SIS spreading process, the mean-field model is accurate for large values of the infection rate for any graph, while for infection rates close to the epidemic threshold, there is considerable difference between the response of the mean-field model and the exact model. Additionally, studies have shown that mean-field SIS models fail to explain the existence of a stable, disease-free, absorbing state [37].

If the initial states are seeded according to an uncorrected distribution, i.e., at the initial time (23) is actually exact, then the mean-field model performs fairly accurately during the early stages of system response. The reason for this is that nodes are poorly correlated at the early stage but become more and more correlated as time goes on. Consequently, accuracy of the transient response of mean-field models has been reported in [38] for the SIS spreading process. The steady-state solution of the mean-field models is also important. For example, the steady-state solution of SIS model belongs to the metastable state in the SIS epidemic process [12]. If accuracy is of greater concern, then higher-order closure techniques can be used. However, this will result in a much larger state-space size. Alternatively, GEMF has the smallest state-space size to describe the spreading process of the type considered in this paper. Any further reduction of the state space essentially implies adopting approximation of the network structure.

One of the great benefits of the GEMF model is its analytical tractability. The SIS mean-field model suggests that the epidemic threshold is the inverse of the spectral radius of the contact network [12]. Finding relationships between spectral properties of underlying network layers and the spreading process is a problem of great interest. In particular, optimal design of some network layers given other network layers is very important from a technological viewpoint. For example, Sahneh and Scoglio [39] used a mean-field SAIS model to find optimal topology of the information dissemination network given a contact network to reduce the impact of an epidemic.

VI. Case Studies

In this section, we show that GEMF can reproduce the N-Intertwined SIS model [12] and the SIR model [14]. Furthermore, the section develops an SAIS model with information dissemination and a model for a scenario where two pathogens are spreading in a host population.

A. SIS N-Intertwined Model

The SIS model, explained in Section II-A, has $M = 2$ number of compartments. The epidemic parameters are the infection rate β and the curing rate δ. In this model, the interaction is only through the contact graph, where "*infected*" is the influencer compartment. Hence, $L = 1$ and $q_1 = 2$. The transition rate graphs for the SIS model are shown in Fig. 4. The adjacency matrices corresponding to the nodal and edge-based transition rate graphs follow from Fig. 4

$$A_\delta = \begin{bmatrix} 0 & 0 \\ \delta & 0 \end{bmatrix} \quad A_\beta = \begin{bmatrix} 0 & \beta \\ 0 & 0 \end{bmatrix}. \tag{28}$$

Therefore, GEMF (26) suggests the following set of differential equations:

$$\frac{dv_i}{dt} = -Q_\delta^T v_i - \sum\nolimits_{j=1}^{N} a_{ij} v_{j,2} Q_\beta^T v_i \tag{29}$$

for the evolution of the compartment probability vectors, where the Q_δ and Q_β matrices, corresponding to A_δ and A_β, respectively, are

$$Q_\delta = \begin{bmatrix} 0 & 0 \\ -\delta & \delta \end{bmatrix} \quad Q_\beta = \begin{bmatrix} \beta & -\beta \\ 0 & 0 \end{bmatrix}. \tag{30}$$

We can denote the probabilities of being susceptible by S_i and being infected by I_i, i.e., $v_i = [S_i, I_i]^T$. Therefore, the evolution of these probabilities according to GEMF is described as

$$\begin{aligned} \begin{bmatrix} \dot{S}_i \\ \dot{I}_i \end{bmatrix} &= -\begin{bmatrix} 0 & 0 \\ -\delta & \delta \end{bmatrix}^T \begin{bmatrix} S_i \\ I_j \end{bmatrix} \\ &\quad - \left(\sum_{j=1}^{N} a_{ij} I_j \right) \begin{bmatrix} \beta & -\beta \\ 0 & 0 \end{bmatrix}^T \begin{bmatrix} S_i \\ I_j \end{bmatrix} \\ &= \begin{bmatrix} \delta I_i - \beta S_i \left(\sum_{j=1}^{N} a_{ij} I_j \right) \\ -\delta I_i + \beta S_i \left(\sum_{j=1}^{N} a_{ij} I_j \right) \end{bmatrix}. \end{aligned} \tag{31}$$

Since $S_i + I_i = 1$, the differential equation

$$\frac{dI_i}{dt} = -\delta I_i + \beta(1 - I_i) \left(\sum\nolimits_{j=1}^{N} a_{ij} I_j \right) \tag{32}$$

is obtained for I_i and $i \in \{1, \ldots, N\}$, which is exactly the SIS N-Intertwined model in [12].

B. SIR N-Intertwined Model

Youssef and Scoglio [14] developed the SIR N-Intertwined model where each agent can be either "*susceptible*," "*infected*," or "*recovered*." Therefore, the number of compartments in this model is $M = 3$. In this model, a susceptible agent can become infected if it is surrounded by infected agents, and the infection process is characterized by the infection rate β. Furthermore, an "*infected*" agent becomes "*recovered*" with rate δ. Unlike the SIS model, a recovered agent does not become infected again in the SIR model. Similar to SIS, there is only $L = 1$ graph layer and $q_1 = 2$. The transition rate graphs, shown in Fig. 7, illustrate that

$$A_\delta = \begin{bmatrix} 0 & 0 & 0 \\ 0 & 0 & \delta \\ 0 & 0 & 0 \end{bmatrix} \quad A_\beta = \begin{bmatrix} 0 & \beta & 0 \\ 0 & 0 & 0 \\ 0 & 0 & 0 \end{bmatrix}. \tag{33}$$

Therefore, GEMF (26) suggests the following set of differential equations:

$$\frac{dv_i}{dt} = -Q_\delta^T v_i - \sum\nolimits_{j=1}^{N} a_{ij} v_{j,2} Q_\beta^T v_i \tag{34}$$

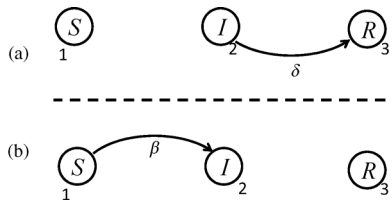

Fig. 7. Transition rate graphs in the SIR model. (a) Nodal transition rate graph. Nodes represent the three compartments "*susceptible*," *infected*," and "*recovered*." Directed link from I to R represents curing process (a nodal transition) weighted by the curing rate $\delta > 0$. (b) Edge-based transition graph of the contact network layer $\mathcal{G}_{\rm c}$. Directed link from S to I represents the infection process (edge-based transition) weighted by the infection rate $\beta > 0$. For the contact network, the influencer compartment is $q_1 = 2$, i.e., "*infected*."

for the evolution of the compartment probability vectors, where the Q matrices are

$$Q_\delta = \begin{bmatrix} 0 & 0 & 0 \\ 0 & \delta & -\delta \\ 0 & 0 & 0 \end{bmatrix} \quad Q_\beta = \begin{bmatrix} \beta & -\beta & 0 \\ 0 & 0 & 0 \\ 0 & 0 & 0 \end{bmatrix} \tag{35}$$

based on (33).

We can denote the probabilities of being susceptible, infected, and recovered by S_i, I_i, and R_i, respectively; i.e., $v_i = [S_i, I_i, R_i]^T$. The evolution of these probabilities are then described as

$$\begin{aligned} \begin{bmatrix} \dot{S}_i \\ \dot{I}_i \\ \dot{R}_i \end{bmatrix} &= - \begin{bmatrix} 0 & 0 & 0 \\ 0 & \delta & -\delta \\ 0 & 0 & 0 \end{bmatrix}^T \begin{bmatrix} S_i \\ I_i \\ R_i \end{bmatrix} \\ &\quad - \left(\sum_{j=1}^{N} a_{ij} I_j \right) \begin{bmatrix} \beta & -\beta & 0 \\ 0 & 0 & 0 \\ 0 & 0 & 0 \end{bmatrix}^T \begin{bmatrix} S_i \\ I_i \\ R_i \end{bmatrix} \\ &= \begin{bmatrix} \beta S_i \left(\sum_{j=1}^{N} a_{ij} I_j \right) \\ -\beta S_i \left(\sum_{j=1}^{N} a_{ij} I_j \right) - \delta I_i \\ \delta I_i \end{bmatrix}. \end{aligned} \tag{36}$$

Since $S_i + I_i + R_i = 1$, the differential equation

$$\begin{aligned} \frac{dI_i}{dt} &= -\delta I_i + \beta(1 - I_i - R_i) \left(\sum_{j=1}^{N} a_{ij} I_j \right) \\ \frac{dR_i}{dt} &= \delta I_i \end{aligned} \tag{37}$$

is obtained for I_i and R_i, which is exactly the SIR N-Intertwined model in [14].

C. SAIS Model With Information Dissemination

Consider the SAIS model in Section II-C, and assume that a susceptible agent becomes alert not only if there are infected individuals in its neighborhood, but also if there are alert individuals in the neighborhood. Also, assume that the latter happens with rate α. Moreover, assume that alert agents can go back to susceptible state with an unalerting rate γ. The interaction is through the contact network $\mathcal{G}_1$, infection information dissemination network $\mathcal{G}_2$, and the alert information dissemination network $\mathcal{G}_3$. For both the contact network and the infection information dissemination network, "*alert*" is the influencer compartment. For the alert information dissemination network, "*alert*" is the influencer compartment. Hence, $L = 3$ and $q_1 = 2$, $q_2 = 2$, $q_3 = 3$.

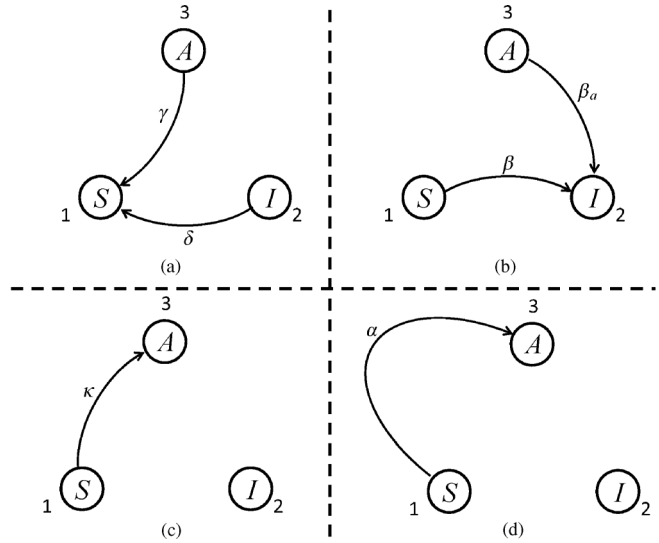

Fig. 8. Transition rate graphs in the SAIS model. (a) Nodal transition rate graph. Nodes represent the three compartments "*susceptible*," "*infected*," and "*alert*." Directed link from I to S represents curing process weighted by the curing rate $\delta > 0$. Directed link from A to S represents the unalerting process weighted by the unalerting rate $\gamma > 0$. (b) Edge-based transition graph of the contact network layer $\mathcal{G}_{\rm c}$. Directed link from S to I represents the infection process (edge-based transition) weighted by the infection rate $\beta > 0$. Directed link from A to I represents the alerted infection process (edge-based transition) weighted by the alerted infection rate $\beta_{\rm a} > 0$. For the contact network, the influencer compartment is $q_1 = 2$, i.e., "*infected*." (c) Edge-based transition graph of the infection information dissemination network layer $\mathcal{G}_{\rm iIDN}$; directed link from S to A represents the alerting process weighted by the alerting rate $\kappa > 0$, For the infection information dissemination network, the influencer compartment is $q_1 = 2$, i.e., "*infected*." (d) Edge-based transition graph of the alert information dissemination network layer $\mathcal{G}_{\rm aIDN}$; directed link from S to A represents the alerting process weighted by the alerting rate $\alpha > 0$, For the alert information dissemination network, the influencer compartment is $q_1 = 3$, i.e., "*alert*."

From Fig. 8

$$A_\delta = \begin{bmatrix} 0 & 0 & 0 \\ \delta & 0 & 0 \\ \gamma & 0 & 0 \end{bmatrix} \quad A_{\beta_1} = \begin{bmatrix} 0 & \beta_0 & 0 \\ 0 & 0 & 0 \\ 0 & \beta_a & 0 \end{bmatrix}$$
$$A_{\beta_2} = \begin{bmatrix} 0 & 0 & \kappa \\ 0 & 0 & 0 \\ 0 & 0 & 0 \end{bmatrix} \quad A_{\beta_3} = \begin{bmatrix} 0 & 0 & \alpha \\ 0 & 0 & 0 \\ 0 & 0 & 0 \end{bmatrix}. \tag{38}$$

Therefore, GEMF (26) suggests the following set of differential equations:

$$\begin{aligned} \frac{dv_i}{dt} &= -Q_\delta^T v_i - \sum_{j=1}^{N} a_{1,ij} v_{j,2} Q_{\beta_1}^T v_i \\ &\quad - \sum_{j=1}^{N} a_{2,ij} v_{j,2} Q_{\beta_2}^T v_i - \sum_{j=1}^{N} a_{2,ij} v_{j,3} Q_{\beta_3}^T v_i \end{aligned} \tag{39}$$

for the evolution of the compartment probability vectors, where the Q matrices are

$$Q_\delta = \begin{bmatrix} 0 & 0 & 0 \\ -\delta & \delta & 0 \\ -\gamma & 0 & \gamma \end{bmatrix} \quad Q_{\beta_2} = \begin{bmatrix} \beta_0 & -\beta_0 & 0 \\ 0 & 0 & 0 \\ 0 & -\beta_a & \beta_a \end{bmatrix}$$
$$Q_{\beta_2} = \begin{bmatrix} \kappa & 0 & -\kappa \\ 0 & 0 & 0 \\ 0 & 0 & 0 \end{bmatrix} \quad Q_{\beta_3} = \begin{bmatrix} \alpha & 0 & -\alpha \\ 0 & 0 & 0 \\ 0 & 0 & 0 \end{bmatrix} \tag{40}$$

according to (38).

Sahneh and Scoglio [39] used a model very similar to (39), where there are only two layers of graphs—namely, the contact network and the infection information dissemination network—to assess the effectiveness of the information networks in reducing the impact of an epidemic. A novel information dissemination metric is introduced that measures the impact of information network on improving the resilience of the system against epidemic spreading. The developed information dissemination metric leads to an analytical solution for the optimal topology of the information network to minimize the impact of an epidemic.

D. Multiple Interacting Pathogen Spreading

The problem of multiple pathogen spreading has recently attracted substantial attention (see, e.g., [40]–[43]). Most models consider a full-cross immunity between pathogens, i.e., a node infected by one type of pathogen cannot be infected with any other type of pathogen at the same time. Beutel *et al.* [42] considered the case where the pathogens also have an interacting effect on each other and spread on the same contact network. In the model introduced by Marceau *et al.* [43], pathogens do not interact, but each pathogen has a separate contact network. In the following, we apply GEMF to develop an individual-based bi-spreading SIS model for epidemic spreading of multiple interacting pathogens, very similar to [42], where each pathogen, as in [43], has a different contact network.

Consider a spreading scenario where two pathogens A and B are spreading among a host population. The contact network for virus A is $\mathcal{G}_A$, while B spreads through $\mathcal{G}_B$. The transition rates for the pathogens depend on each other. For example, the infection process of a susceptible agent by pathogen A has different infection rate if it is already infected by B versus being susceptible to B. In general, we assume the transition rates are $\delta_{A0}, \delta_{A1}, \beta_{A0}, \beta_{A1}$. $\delta_{B0}, \delta_{B1}, \beta_{B0}, \beta_{B1}$. For example, if an agent is infected by A but is not infected by B, then it recovers by rate δ_{A0}. On the other hand, if it is also infected by B, disease A gets cured by rate δ_{A1}. Similar arguments apply for other rate terms.

For this spreading scenario, $M = 4$ compartments can be defined to model the problem. Agent i is in compartment 1 if it is susceptible to both A and B. It is 2 if it is susceptible to A but infected by B. It is 3 if infected by A and susceptible to B. Finally, it is 4 if it is infected by both A and B. The nodal and edge-based transitions are shown in Fig. 9.

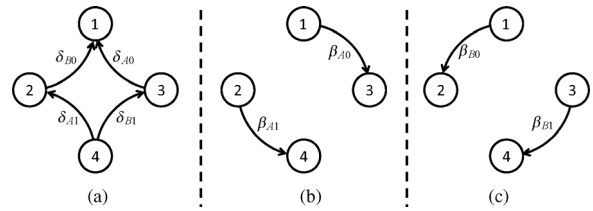

Fig. 9. Transition rate graphs in the bi-spreading SIS model. (a) Nodal transition rate graph. Nodes represent the four compartments "S_AS_B," "S_AI_B," "I_AS_B," and "I_AI_B." Directed links from I_AS_B to S_AS_B and from I_AI_B to S_AI_B represent curing process for virus A weighed with curing rates δ_{A0} and δ_{A1}, respectively, and the directed links from S_AI_B to S_AS_B and from I_AI_B to I_AS_B represents curing process for virus B weighted by the curing rates δ_{B0} and δ_{B1}, respectively. (b) Edge-based transition graph of the contact network layer $\mathcal{G}_A$ for virus A. Directed link from S_AS_B to I_AS_B and from S_AI_B to I_AI_B represents infection process for virus A weighed with infection rates β_{A0} and β_{A1}, respectively. For the contact network $\mathcal{G}_A$, the influencer compartment is $q_A = 3, 4$, i.e., I_AS_B and I_AI_B. (c) Edge-based transition graph of the contact network layer $\mathcal{G}_B$ for virus B. Directed link from S_AS_B to S_AI_B and from I_AS_B to I_AI_B represents infection process for virus B weighed with infection rates β_{B0} and β_{B1}, respectively. For the contact network $\mathcal{G}_B$, the influencer compartment is $q_B = 2, 4$, i.e., S_AI_B and I_AI_B.

It follows from Fig. 9

$$A_\delta = \begin{bmatrix} 0 & 0 & 0 & 0 \\ \delta_{B0} & 0 & 0 & 0 \\ \delta_{A0} & 0 & 0 & 0 \\ 0 & \delta_{A1} & \delta_{B1} & 0 \end{bmatrix} \quad A_{\beta_A} = \begin{bmatrix} 0 & 0 & \beta_{A0} & 0 \\ 0 & 0 & 0 & \beta_{A1} \\ 0 & 0 & 0 & 0 \\ 0 & 0 & 0 & 0 \end{bmatrix}$$
$$A_{\beta_B} = \begin{bmatrix} 0 & \beta_{B0} & 0 & 0 \\ 0 & 0 & 0 & 0 \\ 0 & 0 & 0 & \beta_{B1} \\ 0 & 0 & 0 & 0 \end{bmatrix}. \tag{41}$$

Therefore, GEMF (26) suggests the following set of differential equations:

$$\dot{v}_i = -Q_\delta^T v_i - \sum_{j=1}^{N} a_{A,ij}(v_{j,3} + v_{j,4}) Q_{\beta_A}^T v_i - \sum_{j=1}^{N} a_{B,ij}(v_{j,2} + v_{j,4}) Q_{\beta_B}^T v_i \tag{42}$$

for the evolution of the compartment probability vectors

$$Q_\delta = \begin{bmatrix} 0 & 0 & 0 & 0 \\ -\delta_{B0} & \delta_{B0} & 0 & 0 \\ -\delta_{A0} & 0 & \delta_{A0} & 0 \\ 0 & -\delta_{A1} & -\delta_{B1} & \delta_{A1} + \delta_{B1} \end{bmatrix}$$
$$Q_{\beta_A} = \begin{bmatrix} \beta_{A0} & 0 & -\beta_{A0} & 0 \\ 0 & \beta_{A1} & 0 & -\beta_{A1} \\ 0 & 0 & 0 & 0 \\ 0 & 0 & 0 & 0 \end{bmatrix}$$
$$Q_{\beta_B} = \begin{bmatrix} \beta_{B0} & -\beta_{B0} & 0 & 0 \\ 0 & 0 & 0 & 0 \\ 0 & 0 & \beta_{B1} & -\beta_{B1} \\ 0 & 0 & 0 & 0 \end{bmatrix}. \tag{43}$$

VII. Conclusion

Inspired by existing individual-based epidemic models, we propose the generalized epidemic mean-field model. While using the same common assumptions of most of the existing

individual-based epidemic models, GEMF is capable of modeling more complex scenarios with multiple compartment and multiple network layers. The set of differential equations that fully describes the time evolution of the compartment occupancy probabilities has M^N equations. Even though the system is linear, it is both computationally and analytically intractable, managed through a mean-field type approximation by a set of MN nonlinear differential equations. The latter system, referred to as GEMF, has a simple structure. It is characterized by the Laplacian of the transition rate graphs and the elements of the adjacency matrices of the network layers. A systematic procedure for developing the model is proposed that culminates in the GEMF governing equations (26). The GEMF model is rigorous, allows analytical tractability, and is simple to apply to many specific spreading processes, as shown in the several examples presented in this paper. We believe that the GEMF framework has the potential to allow the development of many different and novel individual-based epidemic models considering new compartments and multiple complex interaction structures.

APPENDIX
DERIVATION OF EXACT MARKOV EQUATION

In this section, we explicitly derive the expression for $\mathbf{Q}$ in (22). The idea is to derive the expression for $E[X(t+\Delta t)]$ as a function of $E[X(t)]$. For this, first we find the expression for the conditional expectation $E[X(t+\Delta t)\,|\,X(t)]$. Then, the expression for $E[X(t+\Delta t)]$ is found by averaging out the conditional. For small values of Δt, we can assume that only one transition happens at each time-step, i.e., starting at network state at time t, the network state can only go to a new state at time $t+\Delta t$ for which only the state of a single node has been changed. Given the network state $X(t)=e_Z$, state $x_i(t)=e_{z_i}$ of each agent i can be determined, and we have

$$e_Z = e_{z_1}\otimes\cdots\otimes e_{z_N}. \tag{A.1}$$

Since only at most one single node can make a transition, the conditional expected value of the network state at time $t+\Delta t$ is

$$E[X(t+\Delta t)\,|\,X(t)=e_Z] = \sum\nolimits_{i=1}^{N} e_{z_1}\otimes\cdots\otimes E[x_i(t+\Delta t)\,|\,X(t)=e_Z]\otimes\cdots\otimes e_{z_N} \tag{A.2}$$

where from (17), the expression for $E[x_i(t+\Delta t)\,|\,X(t)=e_Z]$ is

$$E[x_i(t+\Delta t)\,|\,X(t)=e_Z] = -Q_\delta^T e_{z_i}\Delta t - \sum_{l=1}^{L}\sum_{j=1}^{N} a_{l,ij}1_{\{z_j=q_l\}}Q_{\beta_l}^T e_{z_i}\Delta t + e_{z_i}(t)+\epsilon(\Delta t). \tag{A.3}$$

Averaging all of the possible network states yields the expected value of the network state at time $t+\Delta t$

$$E[X(t+\Delta t)] = \sum\nolimits_{Z=1}^{M^N} E[X(t+\Delta t)\,|\,X(t)=e_Z]\Pr[X(t)=e_Z] = \sum_{Z=1}^{M^N}\left(\sum_{i=1}^{N} e_{z_1}\otimes\cdots\otimes E[x_i(t+\Delta t)\,|\,X(t)=e_Z]\otimes\cdots\otimes e_{z_N}\right)\Pr[X(t)=e_Z]. \tag{A.4}$$

Substituting for $E[x_i(t+\Delta t)\,|\,X(t)=e_Z]$ from (A.3), $E[X(t+\Delta t)]$ is deduced to be

$$E[X(t+\Delta t)] = -\mathbf{Q}_\delta^T E[X(t)]\Delta t - \sum_{l=1}^{L}\mathbf{Q}_{\beta_l}^T E[X(t)]\Delta t + E[X(t)] + o(\Delta t) \tag{A.5}$$

where

$$\mathbf{Q}_\delta = \sum\nolimits_{i=1}^{N} I_{M\times M}\otimes\cdots\otimes Q_\delta\otimes\cdots\otimes I_{M\times M}$$

and $\mathbf{Q}_{\beta_l}$ is such that its Zth column is

$$\mathrm{col}(\mathbf{Q}_{\beta_l},Z) = \sum\nolimits_{i=1}^{N} e_{z_1}\otimes\cdots\otimes\left(\sum_{j=1}^{N} a_{l,ij}1_{\{z_j=q_l\}}Q_{\beta_l}e_{z_i}\right)\otimes\cdots\otimes e_{z_N}. \tag{A.6}$$

By letting $\Delta t\to 0$ in (A.5), the time evolution of $E[X]$ can be fully described by

$$\frac{d}{dt}E[X] = -\mathbf{Q}^T E[X] \tag{A.7}$$

where $\mathbf{Q}$ is defined as

$$\mathbf{Q} = \mathbf{Q}_\delta + \sum_{l=1}^{L}\mathbf{Q}_{\beta_l}. \tag{A.8}$$

The differential equation (A.7) is the exact Markov equation.

REFERENCES

[1] J. Kephart and S. White, "Directed-graph epidemiological models of computer viruses," in *Proc. Soc. Symp. Res. Security Privacy*, May 1991, pp. 343–359.

[2] J. Kleinberg, "Computing: The wireless epidemic," *Nature*, vol. 449, no. 7160, pp. 287–288, 2007.

[3] M. Meisel, V. Pappas, and L. Zhang, "A taxonomy of biologically inspired research in computer networking," *Comput. Netw.*, vol. 54, no. 6, pp. 901–916, 2010.

[4] A. Barabási and Z. Oltvai, "Network biology: Understanding the cell's functional organization," *Nature Rev. Genetics*, vol. 5, no. 2, pp. 101–113, 2004.

[5] C. Lindemann and A. Thümmler, "Performance analysis of the general packet radio service," *Comput. Netw.*, vol. 41, no. 1, pp. 1–17, 2003.

[6] C. Riddalls, S. Bennett, and N. Tipi, "Modelling the dynamics of supply chains," *Int. J. Syst. Sci.*, vol. 31, no. 8, pp. 969–976, 2000.

[7] N. Bailey, *The Mathematical Theory of Infectious Diseases and Its Applications*. London, U.K.: Griffin, 1975.

[8] Y. Moreno, R. Pastor-Satorras, and A. Vespignani, "Epidemic outbreaks in complex heterogeneous networks," *Eur. Phys. J. B, Cond. Matter Complex Syst.*, vol. 26, pp. 521–529, 2002.

[9] R. Pastor-Satorras and A. Vespignani, "Epidemic dynamics and endemic states in complex networks," *Phys. Rev. E*, vol. 63, no. 6, p. 066117, May 2001.

[10] Y. Wang, D. Chakrabarti, C. Wang, and C. Faloutsos, "Epidemic spreading in real networks: An eigenvalue viewpoint," in *Proc. 22nd Int. Symp. Rel. Distrib. Syst.*, 2003, pp. 25–34.
[11] M. Keeling and K. Eames, "Networks and epidemic models," *J. Royal Soc. Interface*, vol. 2, no. 4, pp. 295–307, 2005.
[12] P. Van Mieghem, J. Omic, and R. Kooij, "Virus spread in networks," *IEEE/ACM Trans. Netw.*, vol. 17, no. 1, pp. 1–14, Feb. 2009.
[13] A. Ganesh, L. Massoulie, and D. Towsley, "The effect of network topology on the spread of epidemics," in *Proc. IEEE INFOCOM*, 2005, vol. 2, pp. 1455–1466.
[14] M. Youssef and C. Scoglio, "An individual-based approach to SIR epidemics in contact networks," *J. Theoret. Biol.*, vol. 283, no. 1, pp. 136–144, 2011.
[15] S. Karlin and H. Taylor, *A Second Course in Stochastic Processes*. New York: Academic, 1981.
[16] P. Van Mieghem, *Performance Analysis of Communications Networks and Systems*. Cambridge, U.K.: Cambridge Univ. Press, 2006.
[17] P. Erdös and A. Rényi, *On the Evolution of Random Graphs*. Budapest, Hungary: Akad. Kiadó, 1960.
[18] A. Barabási and R. Albert, "Emergence of scaling in random networks," *Science*, vol. 286, no. 5439, pp. 509–512, 1999.
[19] J. Doyle, D. Alderson, L. Li, S. Low, M. Roughan, S. Shalunov, R. Tanaka, and W. Willinger, "The "robust yet fragile" nature of the Internet," in *Proc. Nat. Acad. Sci.*, 2005, vol. 102, no. 41, p. 14497.
[20] J. Shao, S. Buldyrev, S. Havlin, and H. Stanley, "Cascade of failures in coupled network systems with multiple support-dependence relations," *Phys. Rev. E*, vol. 83, no. 3, p. 036116, 2011.
[21] C. D. Brummitt, R. M. D'Souza, and E. A. Leicht, "Suppressing cascades of load in interdependent networks," *Proc. Nat. Acad. Sci.*, vol. 109, no. 12, pp. E680–E689, 2012.
[22] O. Yağan, D. Qian, J. Zhang, and D. Cochran, "Optimal allocation of interconnecting links in cyber-physical systems: Interdependence, cascading failures, and robustness," *IEEE Trans. Parallel Distrib. Syst.*, vol. 23, no. 9, pp. 1708–1720, Sep. 2012.
[23] S. Funk and V. Jansen, "Interacting epidemics on overlay networks," *Phys. Rev. E*, vol. 81, no. 3, p. 036118, 2010.
[24] M. Dickison, S. Havlin, and H. Stanley, "Epidemics on interconnected networks," *Phys. Rev. E*, vol. 85, no. 6, p. 066109, 2012.
[25] A. Saumell-Mendiola, M. A. Serrano, and M. Boguñá, "Epidemic spreading on interconnected networks," *Phys. Rev. E*, vol. 86, p. 026106, Aug. 2012.
[26] Y. Wang and G. Xiao, "Effects of interconnections on epidemics in network of networks," in *Proc. 7th WiCOM*, Sep. 2011, pp. 1–4.
[27] O. Yağan and V. Gligor, "Analysis of complex contagions in random multiplex networks," *Phys. Rev. E*, vol. 86, no. 3, p. 036103, 2012.
[28] F. Sahneh and C. Scoglio, "Epidemic spread in human networks," in *Proc. IEEE Conf. Decision Control*, 2011, pp. 3008–3013.
[29] W. Richoux and G. Verghese, "A generalized influence model for networked stochastic automata," *IEEE Trans. Syst., Man, Cybern., A, Syst. Humans*, vol. 41, no. 1, pp. 10–23, Jan. 2011.
[30] P. Van Mieghem, *Graph Spectra for Complex Networks*. Cambridge, U.K.: Cambridge Univ. Press, 2011.
[31] S. Ross, *Stochastic Processes*. New York, NY, USA: Wiley, 1983, vol. 23.
[32] C. Gardiner, *Handbook of Stochastic Methods: For Physics, Chemistry and the Natural Sciences*. Berlin, Germany: Springer, 2004.
[33] M. Taylor, P. Simon, D. Green, T. House, and I. Kiss, "From Markovian to pairwise epidemic models and the performance of moment closure approximations," *J. Math. Biol.*, vol. 64, no. 6, pp. 1021–1042, 2012.
[34] E. Cator and P. Van Mieghem, "Second-order mean-field susceptible-infected-susceptible epidemic threshold," *Phys. Rev. E*, vol. 85, no. 5, p. 056111, 2012.
[35] S. C. Ferreira, C. Castellano, and R. Pastor-Satorras, "Epidemic thresholds of the susceptible-infected-susceptible model on networks: A comparison of numerical and theoretical results," arXiv:1206.6728v1, 2012.
[36] C. Li, R. van de Bovenkamp, and P. V. Mieghem, "The SIS mean-field n-intertwined and Pastor-Satorras & Vespignani approximation: A comparison," *Phys. Rev. E*, vol. 86, no. 2, p. 026116, 2012.
[37] P. Van Mieghem, "The N-intertwined SIS epidemic network model," *Computing*, vol. 93, no. 2–4, pp. 147–169, 2011.
[38] Z. Chen and C. Ji, "Spatial-temporal modeling of malware propagation in networks," *IEEE Trans. Neural Netw.*, vol. 16, no. 5, pp. 1291–1303, Sep. 2005.
[39] F. Sahneh and C. Scoglio, "Optimal information dissemination in epidemic networks," in *Proc. IEEE Conf. Decision Control*, 2012, to be published.
[40] M. Newman, "Threshold effects for two pathogens spreading on a network," *Phys. Rev. Lett.*, vol. 95, no. 10, p. 108701, 2005.
[41] M. Lipsitch, C. Colijn, T. Cohen, W. Hanage, and C. Fraser, "No coexistence for free: Neutral null models for multistrain pathogens," *Epidemics*, vol. 1, no. 1, p. 2, 2009.
[42] A. Beutel, B. Prakash, R. Rosenfeld, and C. Faloutsos, "Interacting viruses in networks: Can both survive?," in *Proc. 18th ACM SIGKDD Int. Conf. Knowl. Discov. Data Mining*, 2012, pp. 426–434.
[43] V. Marceau, P. Noël, L. Hébert-Dufresne, A. Allard, and L. Dubé, "Modeling the dynamical interaction between epidemics on overlay networks," *Phys. Rev. E*, vol. 84, no. 2, p. 026105, 2011.

Faryad Darabi Sahneh (M'12) received the B.S. degree in mechanical engineering from Amirkabir University of Technology (Tehran Polytechnic), Tehran, Iran, in 2008, the M.S. degree in mechanical engineering from Kansas State University, Manhattan, KS, USA, in 2010, and is currently pursuing the Ph.D. degree in electrical and computer engineering at Kansas State University.

He is interested in research at the intersection of mathematical modeling, network science, and control theory with application to biological and social complex systems.

Caterina M. Scoglio (M'12) received the Dr.Eng. degree in electronics engineering from the "Sapienza" Rome University, Rome, Italy, in 1987.

She has been an Associate Professor with the Department of Electrical and Computer Engineering, Kansas State University, Manhattan, KS, USA, since 2005. Before joining Kansas State University, she worked with the Fondazione Ugo Bordoni, Rome, Italy, from 1987 to 2000, and at the Georgia Institute of Technology, Atlanta, GA, USA, from 2000 to 2005. Her main research interests include the modeling and analysis of complex networks, with applications in epidemic spreading and power grids.

Piet F. A. Van Mieghem (M'02) received the Master's and Ph.D. degrees in electrical engineering from the Katholieke Universiteit Leuven, Leuven, Belgium, in 1987 and 1991, respectively.

He has been a Professor with the Delft University of Technology, Delft, The Netherlands, since 1998. Before joining Delft, he worked with the Interuniversity Microelectronics Centre (IMEC), Heverlee, Belgium, from 1987 to 1991. During 1993 to 1998, he was a member of the Alcatel Corporate Research Center, Antwerp, Belgium. He was a Visiting Scientist with the Department of Electrical Engineering, Massachusetts Institute of Technology (MIT), Cambridge, MA, USA, from 1992 to 1993, and a Visiting Professor with the Department of Electrical Engineering, University of California, Los Angeles, (UCLA), CA, USA, in 2005, and with the Center of Applied Mathematics, Cornell University, Ithaca, NY, USA, in 2009. He is the author of three books: *Performance Analysis of Communications Networks and Systems* (Cambridge University Press, 2009), *Data Communications Networking* (Techne Press, 2006), and *Graph Spectra for Complex Networks* (Cambridge University Press, 2012). His main research interests lie in the modeling and analysis of complex networks (such as biological, brain, social, infrastructural networks, etc.) and in new Internet-like architectures and algorithms for future communications networks.

He was member of the editorial board of Computer Networks (2005–2006) and of the IEEE/ACM Transactions on Networking (2008–2012). Currently, he serves on the editorial board of the OUP journal of Complex Networks, Computer Communications and the Journal of Discrete Mathematics.